

Article

Investigations of Deformation Behavior and Microstructure of Al Tailored Ti–Mo High Temperature Shape Memory Alloys during Isothermal Holding at 393 K

Naoki Nohira *, Yoshiaki Oshita †, Wan-Ting Chiu, Akira Umise, Masaki Tahara and Hideki Hosoda *

Institute of Innovative Research (IIR), Tokyo Institute of Technology, 4259 Nagatsuta-cho, Midori-ku, Yokohama 226-8503, Japan; oshita.y.aa@gmail.com (Y.O.); chiu.w.aa@m.titech.ac.jp (W.-T.C.); umise.a.aa@m.titech.ac.jp (A.U.); tahara.m.aa@m.titech.ac.jp (M.T.)

* Correspondence: nohira.n.aa@m.titech.ac.jp (N.N.); hosoda.h.aa@m.titech.ac.jp (H.H.)

† Current address: Toyota Motor Corporation, Toyota 471-8571, Japan.

Abstract: To utilize β -Ti based high temperature (HT) shape memory alloys (SMAs), a high Al concentration of 14 mol% was designed for sufficient suppressing the undesired ω -phase. HTSMA exhibits shape memory effect (SME) above 373 K, and thus the operating temperature is over 373 K. However, the SME and the mechanical properties of most β -Ti SMAs deteriorate after holding at elevated temperatures due to the ω -embrittlement. The Ti-4.5Mo-14Al alloy (mol%) and the Ti-6Mo-7Al alloy as a comparison, both of which possess the identical reverse martensitic transformation start temperature of 407 K, were isothermally held at 393 K for up to 360 ks, and deformation behaviors and microstructures were investigated. It was found that after the isothermal holding, the deformation behavior of the Ti-6Mo-7Al alloy altered significantly; on the other hand, that of the Ti-4.5Mo-14Al alloy remained almost intact. Transmission electron microscopy observations revealed that the isothermal ω -phase (ω_{iso}) was successfully suppressed in the Ti-4.5Mo-14Al alloy, while the ω_{iso} phase grew in Ti-6Mo-7Al alloy. Moreover, the isothermal α'' -phase coexisted in the Ti-4.5Mo-14Al alloy. It is concluded that a high Al concentration is a crucial prerequisite in the practical β -Ti HTSMAs. The presented design could be a useful guideline for developing Ti SMAs with comparable Mo- and Al-equivalents.

Keywords: high temperature shape memory alloys; Ti–Mo–Al; deformation behavior; microstructure; isothermal α'' phase; isothermal ω phase



Citation: Nohira, N.; Oshita, Y.; Chiu, W.-T.; Umise, A.; Tahara, M.; Hosoda, H. Investigations of Deformation Behavior and Microstructure of Al Tailored Ti–Mo High Temperature Shape Memory Alloys during Isothermal Holding at 393 K. *Micro* **2022**, *2*, 113–122. <https://doi.org/10.3390/micro2010007>

Academic Editor: Carlo Santulli

Received: 5 January 2022

Accepted: 20 January 2022

Published: 25 January 2022

Publisher's Note: MDPI stays neutral with regard to jurisdictional claims in published maps and institutional affiliations.



Copyright: © 2022 by the authors. Licensee MDPI, Basel, Switzerland. This article is an open access article distributed under the terms and conditions of the Creative Commons Attribution (CC BY) license (<https://creativecommons.org/licenses/by/4.0/>).

1. Introduction

To date, the conventional NiTi (Nitinol) shape memory alloys (SMAs) have been widely put into practice in various industrial communities [1]. Nevertheless, the martensitic transformation temperature of Nitinol, which is below 373 K, has impeded its applicability for high-temperature usages [2,3]. Much effort has thus been put into studying new high-temperature shape memory alloys (HTSMAs) towards the high-temperature applications above 373 K [4,5]. Among the HTSMAs, the metastable β -Ti based SMAs (called β -Ti SMAs), which possess the advantage of being relatively lightweight, meet the fundamental weight-reduction requirements for the applications of the aircraft materials in the aerospace industry [6]. Additionally, the β -Ti SMAs, which further perform excellent corrosion resistance, are a promising candidate for realizing the HTSMAs applications.

To utilize the β -Ti alloys as HTSMAs, essential requirements, such as possessing shape recovery behavior at relatively high operating temperature and being stable at the relatively high operation temperature, are demanded. It is widely known that various metastable β -Ti based alloys suffer from embrittlement, which is brought about by ω -embrittlement, and is generated as the alloys are kept at warm temperatures. Here, ω -embrittlement could be attributed to the formation and growth of the Ti-rich isothermal ω (ω_{iso}) phase in the matrix

of the parent β phase. In addition, the appearance of the ω_{iso} phase further results in a deterioration of the mechanical properties and a reduction of the martensitic transformation temperature [7,8]. Therefore, suppression of the ω -embrittlement is urgently demanded.

Ti–Ta based alloys have been widely investigated for the β -Ti based HTSMAs, since they merely slightly suffer from property deterioration, which is brought about by the ω_{iso} phase [3,9,10]. Moreover, the Al-tailored ternary Ti–Ta–Al alloys have also been greatly studied to further inhibit the growth and formation of the ω_{iso} phase [11]. However, the martensitic transformation temperature was reduced along with the introduction of the Al element and aging treatments to the Ti–Ta based alloys, while the suppression of the undesired ω_{iso} phase was not able to be completely achieved [12]. Moreover, a small shape recovery strain, which stems from the small lattice deformation strain of approximately 3% [13], remains another critical issue.

In view of the difficulties mentioned above, a guideline for the developments of the β -Ti HTSMAs, which perform larger shape recovery strain and small existence of the ω_{iso} phase than the Ti–Ta based alloys, was constructed in this work. Since both Mo and Al serve as the standard elements for the calculation of the equivalent of various additive elements as $[\text{Mo}]_{\text{eq}}$ and $[\text{Al}]_{\text{eq}}$, respectively [2], the ternary Ti–Mo–Al alloy investigated in this study is considered as a prototype for the basic research of the β -Ti SMAs. Therefore, the standard model, which is composed of the typical β (bcc) stabilizing elements of Mo and the α (hcp) stabilizing elements of Al, was designed for tailoring the fundamental mechanical properties and the functionalities of the β -Ti SMAs. Additionally, the Ti–Mo binary alloy, which performs a martensitic transformation start temperature (M_s) near room temperature (RT), exhibits a large lattice deformation strain of 8.5% [14]. The relatively large lattice deformation strain among the various β -Ti based alloys allows them to be potential candidates for the applications toward the β -Ti HTSMAs.

Concerning the shape memory property of the Ti–Mo–Al alloys, Sasano et al. [15] reported the shape memory effect of the Ti-12Mo-3Al (mass%) alloy. A systematic study with various Mo and Al addition concentrations was carried out afterward, claiming that the shape memory effect (SME) was realized in some specimens among the Ti-5Mo-(6–7)Al, Ti-6Mo-(3–8)Al, and Ti-6Mo-(3–8)Al (mol%) alloys [16]. Our research group also discovered that the deformation behavior of the Ti-6Mo-8Al (mol%) alloy altered significantly via specific aging treatments, and it was further suggested that these changes could be ascribed to the existence of the ω_{iso} phase [17].

According to the abovementioned literature, to date, the Al alloying concentration for the ternary Ti–Mo–Al alloys has been restricted in the range of 3–8 mol% for the investigations of their SME and martensitic transformation; in addition, the deformation behavior was deteriorated by certain aging treatment. Since the deteriorated deformation behavior could be ascribed to the existence of the ω_{iso} phase, it thus suggests that the alloying amount of Al at approximately 8 mol% (4.5 mass%) could be insufficient for the suppression of the ω_{iso} phase. A relatively high alloying amount of Al to the β -Ti SMAs, which was designated for the applications of the HTSMAs, was therefore carried out in this study for the suppression of the ω_{iso} phase.

In light of the aforementioned conventional difficulties and requirements, the comparatively high Al alloying concentration of the Ti-4.5Mo-14Al (mol%) alloy, which possesses the reverse martensitic transformation temperature (A_s) at approximately 400 K, was proposed and prepared in this work accordingly. In addition to the Ti-4.5Mo-14Al (mol%) alloy, an alloy with a composition of Ti-6Mo-7Al (mol%), possessing an identical A_s to the Ti-4.5Mo-14Al alloy, was also fabricated for the purpose of comparisons. For achieving the applications towards the HTSMAs, the effect of isothermal holding at 393 K, which is near the operating temperature of HTSMAs on microstructure and deformation behavior, was studied in this work.

2. Materials and Methods

The nominal compositions used in this study were Ti-6Mo-7Al and Ti-4.5Mo-14Al (mol%). The raw materials with a purity of 99.99% for Ti, 99.9% for Mo, and 99.99% for Al were used. Ingots of 8 g were prepared by arc melting method in Ar-1 vol.% H₂ with a non-consumable W-electrode. The ingots were sealed in a quartz tube under an Ar atmosphere, homogenized at 1273 K for 7.2 ks, and then quenched in water.

The homogenized ingots were hot-rolled at 1273 K and cold-rolled into sheets with a thickness of about 0.3 mm. After that, the specimens were solution-treated at 1273 K for 1.8 ks in Ar atmosphere, followed by iced-water quenching. Hereafter, the solution-treated specimens are referred to as “ST” specimens. The maximum oxygen concentration in the ST specimen measured by the inert gas fusion method (EMGA-830, HORIBA, Ltd., Kyoto, Japan) was 0.06 mass%. Thereafter, the effect of oxygen shall not be considered.

Differential scanning calorimetry (DSC; DSC-60 Plus, Shimadzu Corporation, Kyoto, Japan) was performed to evaluate transformation temperatures. A DSC was used for the measurement. The measurement range was 173–523 K, and the heating and cooling rates were ± 10 K/min under Ar atmosphere. The test samples were disk-shaped ST specimens of $\varnothing 3$ mm. Based on the A_s obtained from DSC measurements, the ST specimens were isothermally held for 3.6 ks, 36 ks, and 360 ks, respectively, in a furnace at 393 K, which is about 10 K lower than the measured A_s . The isothermal-treated sample are denoted as “x ks”, e.g., Ti-4.5Mo-14Al 36 ks.

X-ray diffraction measurements (XRD; X'Pert-PRO-MPD, Malvern PANalytical, Malvern, UK) were conducted for phase identification. The measurements were carried out within $2\theta = 20\text{--}120^\circ$ at room temperature (RT; 295 ± 2 K) by a CuK α radiation. A standard Si plate was used to correct for systematic errors.

Scanning electron microscope (SEM; SU5000, Hitachi High-Tech Corporation, Tokyo, Japan) and transmission electron microscope (TEM; JEM-2100, 2100F, JEOL Ltd., Tokyo, Japan) were used for microstructural observations. Samples for SEM were electropolished at about 233 K in a solution of perchloric acid, butanol, and methanol with a volume ratio of 1:6:10. Samples for TEM were disk-shaped specimens of $\varnothing 3$ mm, prepared by twin-jet polishing at about 223 K using a solution of hydrofluoric acid, sulfuric acid, and methanol with a volume ratio of 2:5:93.

Tensile tests were performed to evaluate the mechanical properties. An Instron-type universal testing machine (Autograph AG-X plus 5 kN, Shimadzu Corporation, Kyoto, Japan) was used. The tensile direction was parallel to the cold-rolling direction, and the measurement was carried out until fractures of the samples. The test temperature was set at RT, and the strain rate was set at $8.3 \times 10^{-4} \text{ s}^{-1}$. The samples were dog-bone shaped with a gauge width of 2 mm and length of 10 mm, respectively. Displacement was measured by tracking a marker attached to the specimen by using a video-type non-contact extensometer TRViewX attached to the testing machine.

To evaluate the shape memory properties, tensile tests with loading–unloading cycles were conducted. The testing machine and specimens described above were used for the measurements. The specimens were pre-strained to 4%, unloaded, and then heated up to approximately 500 K by using a heat gun. The amount of shape recovery was measured from the displacement of the crosshead position.

3. Results and Discussion

3.1. Microstructure and Shape Memory Properties of ST Specimens

Figure 1 shows the DSC curves of the ST specimens of both the (a) Ti-4.5Mo-14Al and (b) Ti-6Mo-7Al alloys in the heating process. The endothermic peaks were observed clearly in both alloys, which correspond to the reverse martensitic transformation start temperature (A_s) from α'' to β phase. A_s were read from the DSC curves by constructing the tangent lines. Both the values of A_s were at approximately 407 K, which were the same for these two alloys. No apparent exothermic peaks corresponding to the forward

martensitic transformation temperatures could be observed in the cooling process in both alloys (not shown).

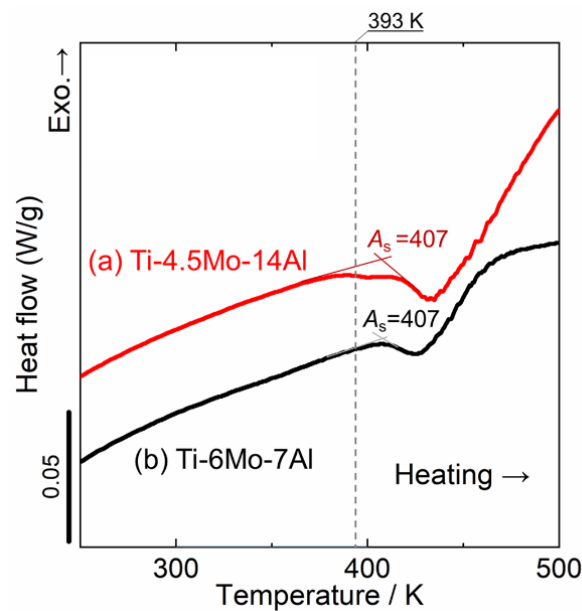


Figure 1. DSC curves of the (a) Ti-4.5Mo-14Al ST and (b) Ti-6Mo-7Al ST specimens in the heating process.

The XRD profiles of the (a) Ti-4.5Mo-14Al ST and (b) Ti-6Mo-7Al ST specimens at RT are shown in Figure 2, respectively. Phase constituents of both ST specimens were the β phase and α'' phase for these two alloys. These results indicate that their M_s is above RT and forward martensitic finish temperature (M_f) is below RT. The absence of a clear peak of forward martensitic transformation in DSC measurements, as is often observed in many β -Ti SMAs, can be attributed to the broad range from M_s to M_f .

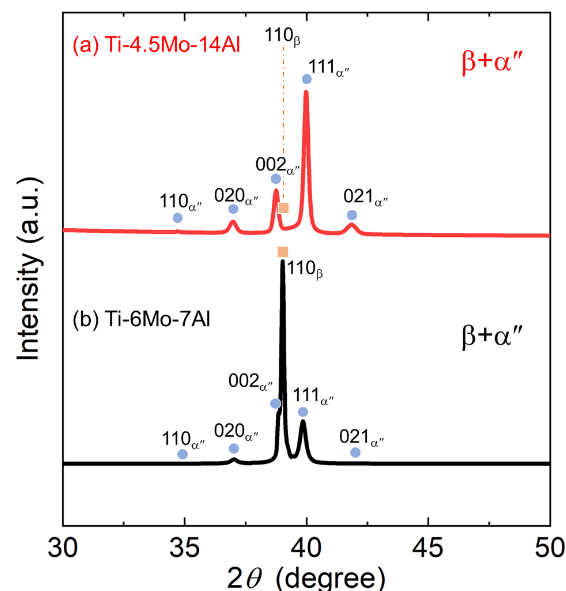


Figure 2. XRD profiles of the (a) Ti-4.5Mo-14Al ST and (b) Ti-6Mo-7Al ST specimens at RT.

Figure 3 shows the SEM images of the (a) Ti-4.5Mo-14Al ST and (b) Ti-6Mo-7Al ST specimens. In both images, equiaxed grains of the β phase were observed. The grain size of the β matrix was about 400 μm . Figure 3 shows the vicinity of the triple points of the grain boundary, indicating the presence of acicular martensitic of the α'' phase near the grain boundaries.

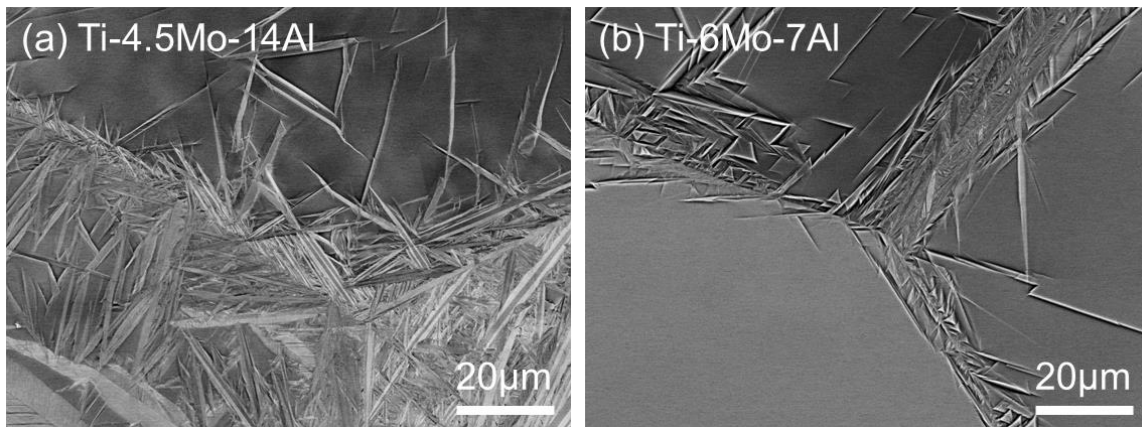


Figure 3. SEM images of the (a) Ti-4.5Mo-14Al ST and (b) Ti-6Mo-7Al ST specimens.

In the Ti-4.5Mo-14Al ST alloy, as shown in Figure 3a, the area fraction of the β phase is low, and the area fraction of the α'' phase is high. On the other hand, in the Ti-6Mo-7Al ST alloy, as shown in Figure 3b, the α'' phase fraction appears to be lower than that of the Ti-4.5Mo-14Al ST alloy. These results were in good agreement with the XRD results as shown in Figure 2. Therefore, although their A_s were similar, the fraction of the α'' phase in the quenched microstructures were slightly different, and qualitatively, the α'' phase was more stable in the Ti-4.5Mo-14Al ST alloy than in that of the Ti-6Mo-7Al alloy. This attributed to the formation of the athermal ω (ω_{ath}), which was less suppressed in the lower Al contained Ti-6Mo-7Al ST alloy than in the higher Al contained Ti-4.5Mo-14Al ST alloy. In the Ti-6Mo-7Al ST alloy, there was relatively less Al, which is also known to be able to suppress the ω_{ath} phase [18,19]; consequently, the ω_{ath} phase inhibited the propagation of martensitic transformation from the β phase to the α'' phase during quenching, and more of the β phase remained, accordingly. The confirmation of ω_{ath} will be described in connection with TEM observation.

To clarify whether these alloys actually perform SME or not, they were subjected to a pre-strain of 4% of tensile stress and were heated after unloading to verify their shape recovery behavior. The obtained stress–strain curves of these two alloys are shown in Figure 4. The red arrows, shown as ϵ_{sme} , indicate the shape recovery strain by SME. The residual strain of about 2.5% after unloading was entirely recovered in both alloys upon heating. These results indicate that both alloys are applicable to the HTSMAs with shape recovery temperatures above 373 K; meanwhile, at least 2.5% of shape recovery strains were achieved.

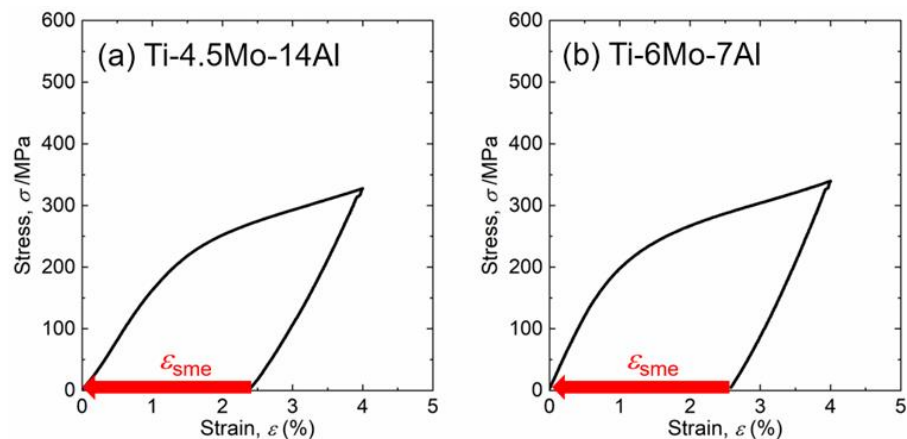


Figure 4. Shape recovery tests of the (a) Ti-4.5Mo-14Al ST and (b) Ti-6Mo-7Al ST specimens. The red arrows, shown as ϵ_{sme} , indicate the shape recovery strain by SME.

3.2. Effect of Isothermal Holding on Mechanical Properties

Figure 5 shows the stress–strain curves of the ST, 3.6 ks, 36 ks, and 360 ks specimens tested at RT. Figure 5a shows the results of the Ti-4.5Mo-14Al alloy, and Figure 5b shows the results for the Ti-6Mo-7Al alloy. A distinct two-stage yielding behavior was observed in both ST specimens. Since the almost perfect SME (nearly 100%) was confirmed by the shape recovery test in both alloys as shown in Figure 4, it can be concluded that the first stage yielding in the stress–strain curves corresponds to the commencement of stress-induced martensitic transformation from the residual β phase to the α'' martensite phase and/or the reorientation of the martensite variant. The second stage yielding corresponds to the commencement of plastic deformation of the reoriented variants. In the following discussion, we focus on the discussion of changes in deformation behavior due to isothermal holding.

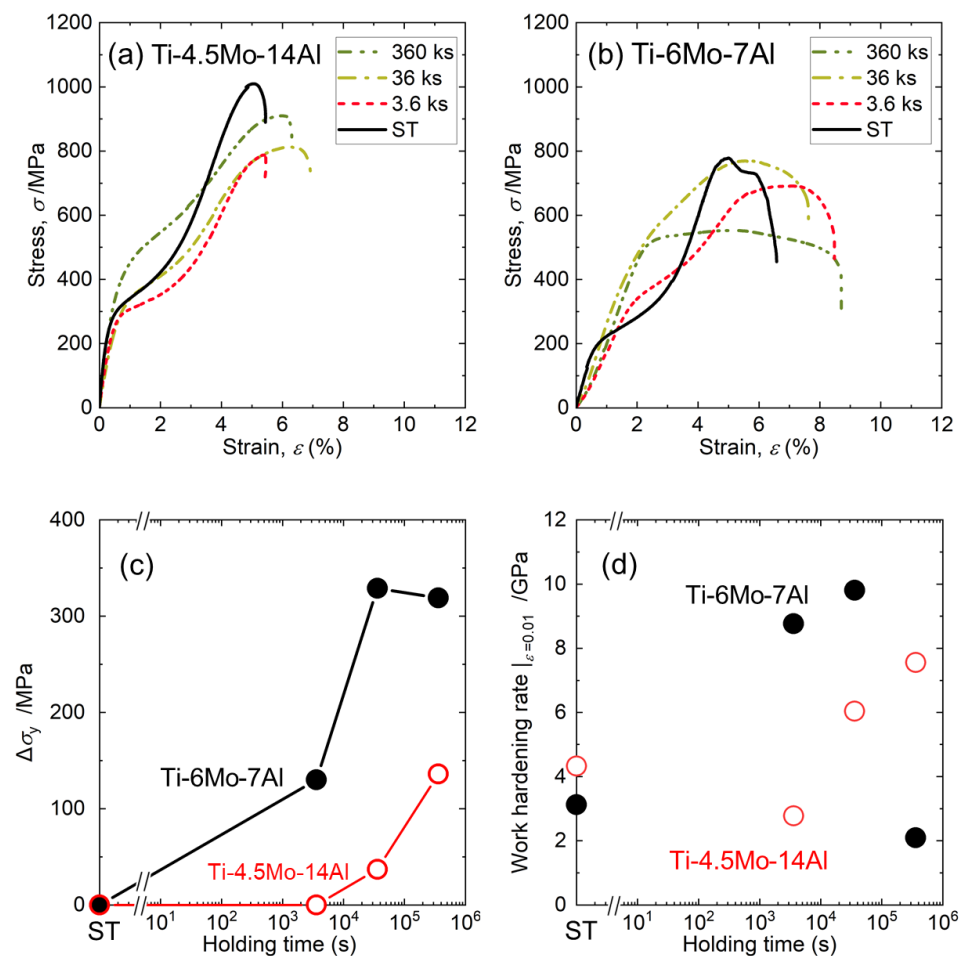


Figure 5. Stress–strain curves of the 393 K held (a) Ti-4.5Mo-14Al and (b) Ti-6Mo-7Al specimens. (c) Increase of yield stress of both specimens held at 393 K as a function of holding time. (d) Work hardening rate at a true strain rate of 0.01 after first yielding of both specimens held at 393 K as a function of holding time. Note that the deviation of the σ_y of different specimens was within 20 MPa (i.e., deviation is smaller than the circle symbols shown).

All the Ti-4.5Mo-14Al alloys by various holding times shown in Figure 5a performed two-stage yielding behavior, even in the Ti-4.5Mo-14Al 360 ks specimen. In addition, the yield stress was slightly higher than that of the ST specimen, while merely little change was found in their deformation behaviors.

On the other hand, the yield stress of the Ti-6Mo-7Al alloy shown in Figure 5b increased in the 3.6 ks alloy compared to the ST alloy, and the two-stage yielding behavior was still found in the 3.6 ks alloy. The two-stage yielding behavior was no longer observed in both Ti-6Mo-7Al 36 ks and 360 ks specimens. Work hardening occurred after yielding in

the Ti-6Mo-7Al 36 ks specimen, whereas almost no work hardening was observed in the 360 ks specimen. Thus, it could be concluded that the isothermal holding at 393 K greatly altered the deformation behavior of the Ti-6Mo-7Al specimens.

To clarify the changing of the yield stress, the increase in yield stress ($\Delta\sigma_y$) in the first stage from the ST specimens for each alloy was plotted against the holding time at 393 K (Figure 5c). Note that the yield stress σ_y was read by the tangent method. The $\Delta\sigma_y$ of the Ti-6Mo-7Al alloy, which exhibited an obvious change in deformation behavior, was 130 MPa at 3.6 ks holding time, 329 MPa at 36 ks holding time, and 319 MPa at 360 ks holding time. Thus, the yield stress of the Ti-6Mo-7Al alloy increased significantly in the early stage of the isothermal holding treatment. On the other hand, $\Delta\sigma_y$ of the Ti-4.5Mo-14Al alloy remained almost unchanged at 3.6 ks, while it changed slightly to 37 MPa at 36 ks and 136 MPa at 360 ks holding times. Therefore, it can be concluded that, in the case of the Ti-4.5Mo-14Al alloy, the change in $\Delta\sigma_y$ increased slightly with holding time, but the change was small.

To clarify the work hardening effect, the work hardening rate ($d\sigma/d\varepsilon$ in true stress-strain curves) at a true strain of 0.01 after first yielding for each alloy was plotted against the holding time at 393 K (Figure 5d). Generally, the work hardening rate of the Ti-4.5Mo-14Al alloy, which exhibited no obvious change in deformation behavior, increased gradually from 0 s to 360 ks holding time, with a certain acceptable deviation. The maximum work hardening rate was observed at the specimen held at 393 K for 360 ks in the case of the Ti-4.5Mo-14Al alloy series. These results suggest that a different work hardening rate should be associated with their change in propagation of stress-induced martensite and/or the reorientation of martensite variant due to isothermal holding. On the other hand, the work hardening rate of the Ti-6Mo-7Al alloy, which exhibited an obvious change in deformation behavior, behaved in a different trend. That is, we observed a maximum work hardening rate at 36 ks and a minimum rate at 360 ks. These results indicate that the deformation mechanism of the Ti-6Mo-7Al alloy series was changed greater than that of the Ti-4.5Mo-14Al alloy series by isothermal holding. As a result, the deformation behavior of the Ti-6Mo-7Al alloy series changed after holding at 393 K. However, the deformation behavior of the Ti-4.5Mo-14Al alloy series with a relatively high amount of Al did not change much even after holding at 393 K for 360 ks. Therefore, the Ti-4.5Mo-14Al alloy is suitable for the applications towards HTSMAs.

3.3. Effect of Isothermal Holding at 393 K on Precipitation Behavior

Figure 6 shows dark-field (DF) images and corresponding selected area diffraction patterns (SADP) of (a) Ti-6Mo-7Al ST, (b) Ti-6Mo-7Al 36 ks, (c) Ti-4.5Mo-14Al ST, and (d) Ti-4.5Mo-14Al 36 ks specimens. It was found that the diffraction spots of the ω phase were apparently observed at $1/3$ and $2/3$ of $\langle 112 \rangle_{\beta^*}$, and additional diffuse scattering was observed at $1/2$ of $\langle 112 \rangle_{\beta^*}$ in all SADPs. The ω spots are distinct in the Ti-6Mo-7Al ST specimen, as shown in Figure 6a. Since the ω phase was formed during quenching, the ω phase is an athermal (diffusionless) ω phase (ω_{ath}). In the Ti-6Mo-7Al alloy, as shown in Figure 6b, the ω phase spots are more distinct than the ST specimen after isothermal holding; additionally, the DF images show that the particles of the ω phase grow obviously large. Since the ω phase grew up during isothermal holding, the ω phase is the isothermal (diffusion) ω phase (ω_{iso}). Then, suppression of the ω_{iso} phase growth is not sufficient in the Ti-6Mo-7Al alloy. The ω_{iso} phase precipitation causes a reduction of martensitic transformation temperature and increase of stress for inducing martensite.

On the other hand, in the Ti-4.5Mo-14Al alloy (Figure 6c,d), there was no obvious change in the spot intensities of the ω phase as well as the particle amount and size of the ω phase after isothermal holding compared to the ST specimen. Then, it can be said that in the Ti-4.5Mo-14Al alloy series, the deformation behavior almost stayed unchanged since the high Al addition sufficiently suppressed the formation of the ω_{ath} phase as well as the formation and growth of the ω_{iso} phase during isothermal holding at 393 K. Thus, it can be concluded that the addition of 14 mol% Al suppressed the formation and growth of both ω_{ath} and ω_{iso} phases.

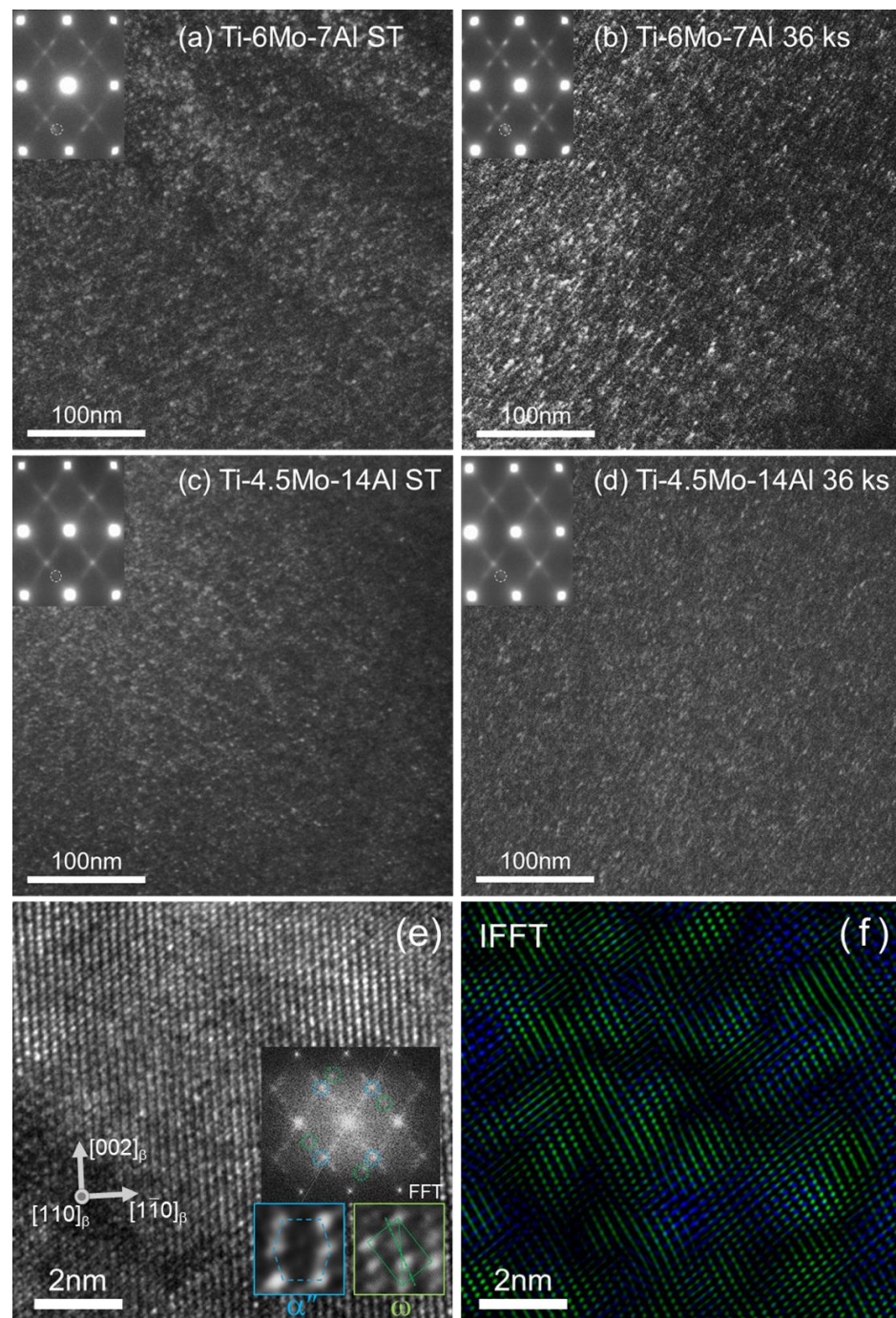


Figure 6. TEM-DF images and the corresponding SADPs from $\mathbf{B} = [110]_{\beta}$ of the (a) Ti-6Mo-7Al ST, (b) Ti-6Mo-7Al 36 ks, (c) Ti-4.5Mo-14Al ST, and (d) Ti-4.5Mo-14Al 36 ks specimens. (e) HRTEM lattice image of Ti-4.5Mo-14Al 36 ks along $[110]_{\beta}$ zone axis. (f) Superimposed IFFT images obtained by selecting the spots shown in the FFT of the inset of (e). (Blue area indicates the α''_{iso} phase; Green area indicates the ω phase).

The position of diffuse scattering corresponds to that of the α'' martensite phase. Similar diffuse scattering in the solution-treated β phase has been reported in several metastable β -Ti alloys [20–23], and it is attributed to the α'' martensite type lattice modulation. After isothermal holding, as shown in Figure 6d, the diffuse scattering was more distinct than the ST specimen. The isothermal α'' (α''_{iso}) phase is known to be a fine α'' phase formed from the lattice modulation via aging treatment (or we say isothermal treatment) [22]. This is in agreement with the results of the present study.

To clarify the distribution of the precipitations in the Ti-4.5Mo-14Al alloy after isothermal holding at 393K for 36 ks, a high-resolution TEM (HRTEM) image along the $[110]_{\beta}$ axis was obtained, as shown in Figure 6e. The fast Fourier transform (FFT) image is also shown in the inset of Figure 6e. Then, the inverse fast Fourier transform (IFFT) images were created from the blue and green circles shown in the FFT image, respectively, and are superimposed in Figure 6f. In the region shown in the blue square, the lattice image shifted with shuffling in the $[\bar{1}10]_{\beta}$ direction, confirming the existence of the α''_{iso} phase. On the other hand, in the region shown in the green square, the collapsed $(\bar{1}11)_{\beta}$ planes were observed, indicating the ω_{iso} phase. In Figure 6f, the IFFT images show that both the ω_{iso} and α''_{iso} phases have a dimension of about 2 nm and were complementarily dispersed. The slight increase of yield stress after isothermal holding in the Ti-4.5Mo-14Al is considered to be related to the increase of α''_{iso} phase precipitates. These details should be further investigated.

It was clarified that mechanical properties of the alloy with α''_{iso} phase were found to be less deteriorated than that of the alloy with ω_{iso} phase. The growth of ω_{iso} phase was suppressed in the Ti-4.5Mo-14Al alloy with high Al composition, and thus, the deformation behavior did not change significantly. Therefore, it can be concluded that Ti–Mo–Al alloys with a higher Al content than that in the already studied low Al composition range are suitable for HTSMAs because the microstructure and mechanical properties do not change considerably during isothermal holding. The results obtained in this study are easily applicable to other Ti-based SMA research by replacement from Mo to $[\text{Mo}]_{\text{eq}}$ and from Al to $[\text{Al}]_{\text{eq}}$. The metastable β phase regions with higher Al content than 10 mol% are worth further investigation for the development of high performance and highly functional shape memory and superelastic alloys.

4. Conclusions

In this study, the Ti–Mo–Al ternary system, which is the basic and standard system in β -Ti alloys, was used for the design guideline to use metastable β -Ti alloy as a high temperature shape memory alloy (HTSMA). The effect of the addition of 14 mol% Al, which is higher than the reported composition range, on the suppression of ω phases, was verified.

For this purpose, the Ti-6Mo-7Al (mol%) alloy and Ti-4.5Mo-14Al (mol%) alloy, which have the same reverse martensitic transformation start temperature (A_s) of 407 K, were isothermally held at 393 K, which is above 373 K and below A_s , for up to 360 ks, and the deformation behavior and microstructure were observed. As a result, the deformation behavior of the Ti-6Mo-7Al alloy changed significantly, and the yield stress increased after 393 K isothermal holding. On the other hand, the deformation behavior of the Ti-4.5Mo-14Al alloy did not change significantly after isothermal holding, and the yield stress increased slightly. HRTEM observations showed that isothermal ω (ω_{iso}) and isothermal α'' (α''_{iso}) phases coexisted after isothermal holding. In comparison to the Ti-6Mo-7Al alloy with ω_{iso} phase growth, the ω_{iso} growth was sufficiently suppressed in the Ti-4.5Mo-14Al alloy, and thus deformation behavior was unchanged after isothermal holding.

The ω_{iso} phase, which caused the change in deformation behavior after isothermal holding, could be suppressed by a higher concentration of Al than the previously studied Al composition range. Furthermore, the composition near Ti-4.5Mo-14Al is promising for HTSMAs. Moreover, the metastable β -Ti phase region with higher Al content or Al equivalent to 10 mol% is worth investigation for the further development of β -Ti SMAs.

Author Contributions: Conceptualization, N.N., Y.O. and H.H.; methodology, N.N. and Y.O.; validation, W.-T.C., A.U., M.T. and H.H.; formal analysis, N.N. and Y.O.; investigation, N.N., Y.O. and W.-T.C.; resources, M.T. and H.H.; data curation, N.N. and W.-T.C.; writing—original draft preparation, N.N.; writing—review and editing, W.-T.C. and H.H.; visualization, N.N.; supervision, W.-T.C., A.U., M.T. and H.H.; project administration, H.H.; funding acquisition, M.T. and H.H. All authors have read and agreed to the published version of the manuscript.

Funding: This work is supported by the Japan Society for the Promotion of Science (JSPS) (KAKENHI 19H02417 and KAKENHI 20K20544).

Institutional Review Board Statement: Not applicable.

Informed Consent Statement: Not applicable.

Data Availability Statement: The data required to reproduce these findings cannot be shared at this time as the data also forms part of an ongoing study.

Conflicts of Interest: The authors declare no conflict of interest.

References

1. Yamauchi, K.; Ohkata, I.; Tsuchiya, K.; Miyazaki, S. *Shape Memory and Superelastic Alloys: Applications and Technologies*; Yamauchi, K., Ohkata, I., Tsuchiya, K., Miyazaki, S., Eds.; Woodhead Publishing: Philadelphia, PA, USA, 2011.
2. Boyer, R.; Welsch, G.; Collings, E.W. *Materials Properties Handbook: Titanium Alloys*; ASM International: Materials Park, OH, USA, 1994.
3. Buenconsejo, P.J.S.; Kim, H.Y.; Hosoda, H.; Miyazaki, S. Shape Memory Behavior of Ti-Ta and Its Potential as a High-Temperature Shape Memory Alloy. *Acta Mater.* **2009**, *57*, 1068–1077. [[CrossRef](#)]
4. Firstov, G.S.; Van Humbeeck, J.; Koval, Y.N. High-Temperature Shape Memory Alloys Some Recent Developments. *Mater. Sci. Eng. A* **2004**, *378*, 2–10. [[CrossRef](#)]
5. Ma, J.; Karaman, I.; Noebe, R.D. High Temperature Shape Memory Alloys. *Int. Mater. Rev.* **2010**, *55*, 257–315. [[CrossRef](#)]
6. Yang, Z.Y.; Zheng, X.H.; Cai, W. Martensitic Transformation and Shape Memory Effect of Ti–V–Al Lightweight High-Temperature Shape Memory Alloys. *Scr. Mater.* **2015**, *99*, 97–100. [[CrossRef](#)]
7. Hickman, B.S. The Formation of Omega Phase in Titanium and Zirconium Alloys: A Review. *J. Mater. Sci.* **1969**, *4*, 554–563. [[CrossRef](#)]
8. Nozoe, F.; Matsumoto, H.; Jung, T.K.; Watanabe, S.; Saburi, T.; Hanada, S. Effect of Low Temperature Aging on Superelastic Behavior in Biocompatible β TiNbSn Alloy. *Mater. Trans.* **2007**, *48*, 3007–3013. [[CrossRef](#)]
9. Buenconsejo, P.J.S.; Kim, H.Y.; Miyazaki, S. Effect of Ternary Alloying Elements on the Shape Memory Behavior of Ti–Ta Alloys. *Acta Mater.* **2009**, *57*, 2509–2515. [[CrossRef](#)]
10. Yi, X.; Sun, K.; Liu, J.; Zheng, X.; Meng, X.; Gao, Z.; Cai, W. Tailoring the Microstructure, Martensitic Transformation and Strain Recovery Characteristics of Ti-Ta Shape Memory Alloys by Changing Hf Content. *J. Mater. Sci. Technol.* **2021**, *83*, 123–130. [[CrossRef](#)]
11. Williams, J.C.; Hickman, B.S.; Leslie, D.H. The Effect of Ternary Additions on the Decomposition of Metastable Beta-Phase Titanium Alloys. *Metall. Trans.* **1971**, *2*, 477–484. [[CrossRef](#)]
12. Buenconsejo, P.J.S.; Kim, H.Y.; Miyazaki, S. Novel β -TiTaAl Alloys with Excellent Cold Workability and a Stable High-Temperature Shape Memory Effect. *Scr. Mater.* **2011**, *64*, 1114–1117. [[CrossRef](#)]
13. Kim, H.Y.; Fukushima, T.; Buenconsejo, P.J.S.; Nam, T.; Miyazaki, S. Martensitic Transformation and Shape Memory Properties of Ti–Ta–Sn High Temperature Shape Memory Alloys. *Mater. Sci. Eng. A* **2011**, *528*, 7238–7246. [[CrossRef](#)]
14. Davis, R.; Flower, H.M.; West, D.R.F. Martensitic Transformations in Ti–Mo Alloys. *J. Mater. Sci.* **1979**, *14*, 712–722. [[CrossRef](#)]
15. Sasano, H.; Suzuki, T. Shape Memory Effect in Ti–Mo–Al Alloys. In Proceedings of the 5th International Conference on Titanium, Munich, Germany, 10–14 September 1984; pp. 1667–1674.
16. Hosoda, H.; Hosoda, N.; Miyazaki, S. Mechanical Properties of Ti–Mo–Al Biomedical Shape Memory Alloys. *Trans. Mater. Res. Soc. Jpn.* **2001**, *26*, 243–246.
17. Hosoda, H.; Taniguchi, M.; Inamura, T.; Kanetaka, H.; Miyazaki, S. Effect of Aging on Mechanical Properties of Ti–Mo–Al Biomedical Shape Memory Alloy. *Mater. Sci. Forum.* **2010**, *654–656*, 2150–2153. [[CrossRef](#)]
18. Sugano, D.; Ikeda, M. The Effect of Aluminum Content on Phase Constitution and Heat Treatment Behavior of Ti–Cr–Al Alloys for Healthcare Application. *Mater. Sci. Eng. C* **2005**, *25*, 377–381. [[CrossRef](#)]
19. Wang, W.; Zhang, X.; Sun, J. Phase Stability and Tensile Behavior of Metastable β Ti–V–Fe and Ti–V–Fe–Al Alloys. *Mater. Charact.* **2018**, *142*, 398–405. [[CrossRef](#)]
20. Tahara, M.; Kim, H.Y.; Inamura, T.; Hosoda, H.; Miyazaki, S. Lattice Modulation and Superelasticity in Oxygen-Added β -Ti Alloys. *Acta Mater.* **2011**, *59*, 6208–6218. [[CrossRef](#)]
21. Zheng, Y.; Williams, R.E.A.; Nag, S.; Banerjee, R.; Fraser, H.L.; Banerjee, D. The Effect of Alloy Composition on Instabilities in the β Phase of Titanium Alloys. *Scr. Mater.* **2016**, *116*, 49–52. [[CrossRef](#)]
22. Tahara, M.; Hasunuma, K.; Ibaki, R.; Inamura, T.; Hosoda, H. Microstructural Evolution in β -Metastable Ti–Mo–Sn–Al Alloy during Isothermal Aging. *Adv. Eng. Mater.* **2019**, *21*, 1900416. [[CrossRef](#)]
23. Li, T.; Lai, M.; Kostka, A.; Salomon, S.; Zhang, S.; Somsen, C.; Dargusch, M.S.; Kent, D. Composition of the Nanosized Orthorhombic O' Phase and Its Direct Transformation to Fine α during Ageing in Metastable β -Ti Alloys. *Scr. Mater.* **2019**, *170*, 183–188. [[CrossRef](#)]